MODELING AND EXTENDING THE RCA MARK II SOUND EFFECTS FILTER

Kurt James Werner *

Cambridge, MA
kurt.james.werner@gmail.com

Ezra J. Teboul †, *Seth Cluett*

Columbia University
New York, NY
ezra@redthunderaudio.com
sc4340@columbia.edu

Emma Azelborn

iZotope, Inc.
Boston, MA
eazelborn@izotope.com

ABSTRACT

We have analyzed the Sound Effects Filter from the one-of-a-kind RCA Mark II sound synthesizer and modeled it as a Wave Digital Filter using the Faust language, to make this once exclusive device widely available. By studying the original schematics and measurements of the device, we discovered several circuit modifications. Building on these, we proposed a number of extensions to the circuit which increase its usefulness in music production.

1. INTRODUCTION

The Mark II synthesizer was the result of an agreement between Columbia University in New York City and the Radio Corporation of America (RCA).[1] RCA began during World War I as a US-government-backed radio monopoly [1], and was by the 1950s a large producer of military and consumer electronics and components. In 1952, RCA engineers Harry Olson and Herbert Belar began developing the Mark I synthesizer at the company's Sarnoff Research Center in Princeton, NJ [2, 3]. After hearing about this three ton vacuum tube synthesizer, two founders of Columbia University's new electronic music center—Vladimir Ussachevsky and Otto Luening—began negotiating for the installation of the second version of the system into their facility in Prentis Hall at W 125th Street in Harlem (a former dairy bottling plant that housed the Heat Transfer Research facility during the Manhattan Project). Today, the Mark II remains bolted to the third floor of what is now Columbia University's Computer Music Center (CMC).

The acquisition of this system marked the beginning of a period of rapid growth and increasing cultural capital for what was then the Columbia-Princeton Electronic Music Center (CPEMC), with an early grant from the Rockefeller Foundation [4–7]. While use of the synthesizer was limited [8], it helped establish the center as one of the world's foremost experimental composition spaces. The Mark II helped place the slowly-institutionalizing east coast electronic music avant-garde within the larger, politicized, American techno-scientific project of the 20th century [9, 10].

Despite being called "a tour-de-force of circuit design" [3], the specifics of the Mark II's circuits have not received scholarly attention. Olson, Belar and Timmens' original discussions are high-level [11–14] and do not always detail the sonic consequences of their choice of specific circuit topologies, components, or interface designs. The processing of the 312 linear feet of paper records in the CPEMC archive remains partial, complicating the task of the scholar [15] who is interested in understanding the synthesizer.

This paper builds on precedents [16–19] mobilizing archival documents and in situ examination to describe and model the four Sound Effects Filter (SEF) units present in the RCA Mark II (§2). Using the schematics, technical documentation, and notes provided for each module of the synthesizer at the time of its delivery, along with measurement and inspection of the circuits themselves, we detail and discuss a modification (§3) made to the SEF units and determine missing component values for both the original circuit and the "mod."[2]. We recap the principles of constant-k circuit design (§4), build a Wave Digital Filter (WDF) model of the SEF (§5), and discuss extensions to the design (§6). §7 concludes.

2. CIRCUIT DESCRIPTION

The original device (Fig. 1, schematic in Fig. 2) comprises a highpass (HP) and a lowpass (LP) section terminated on a resistor R_t. Each section is a "T"-type, with the HP T-section including two capacitors C^HP on top of the "T" and one inductor L^HP on its "stem"; and the LP T-section including two inductors L^LP on top of the "T" and one capacitor C^LP on its "stem."[3]

The two stock controls are 11-position, Mallory-brand, rotary switches: one controlling the highpass cutoff frequency and one controlling the lowpass cutoff frequency. Each rotary controls simultaneously the inductor and capacitor values in its stage. Calling the knob positions $\ell_\mathrm{HP} \in \{1, 2, \cdots, 11\}$ and $\ell_\mathrm{LP} \in \{1, 2, \cdots, 11\}$, we have $C^\mathrm{HP} = C^\mathrm{HP}_{\ell_\mathrm{HP}}$, $L^\mathrm{HP} = L^\mathrm{HP}_{\ell_\mathrm{HP}}$, $C^\mathrm{LP} = C^\mathrm{LP}_{\ell_\mathrm{LP}}$, and $L^\mathrm{LP} = L^\mathrm{LP}_{\ell_\mathrm{LP}}$. The way that the rotary switches create variable capacitances and inductances is shown in Fig. 3. While the capacitors are just switched in and out (other than a wire, essentially $C^\mathrm{HP}_1 = \infty$ and an open circuit, essentially $C^\mathrm{LP}_{11} = 0$), the designers assembled the appropriate inductances as series combinations of multiple inductors. Mechanically, each group of 5 inductors is a single winding around one core, tapped out at appropriate places. Similar to the capacitors, the HP uses an open circuit ($L^\mathrm{HP}_1 = \infty$) and the LP uses a short circuit ($L^\mathrm{LP}_{11} = 0$). The cutoff frequencies in the highpass and lowpass sections are almost identical, and are on average half-octave spaced (6.02 semitones), where the spacing is quite constant (to within ± 0.552 semitones), as shown in Tab. 1.

This original circuit schematic by Robert A. Lynn, provided by RCA to Columbia, is dated March 14th, 1956: its inputs and outputs are designed to be used with input–output impedance match-

---

* This research was conducted during the 1st author's employment at iZotope, Inc., Boston, MA.

† This work was supported by the FACE Foundation's *Etant Donnés* grant for the project "Beyond Circuits."

[1] Columbia-Princeton Electronic Music Center (CPEMC) records 1958–2014, call number MS#1723, Columbia University, box 56.

[2] CPEMC records, Columbia University, box 64.

[3] Interestingly, some more high-level descriptions of the circuit actually show Π-type symmetric sections rather than "T"-type [11].

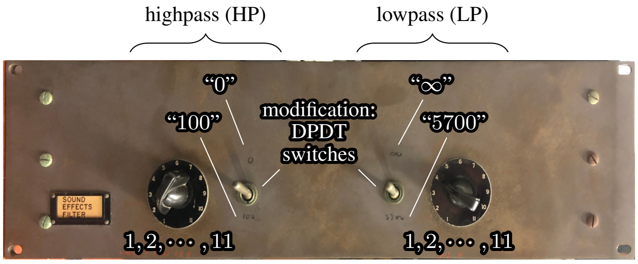

(a) Front panel of SEF #1.

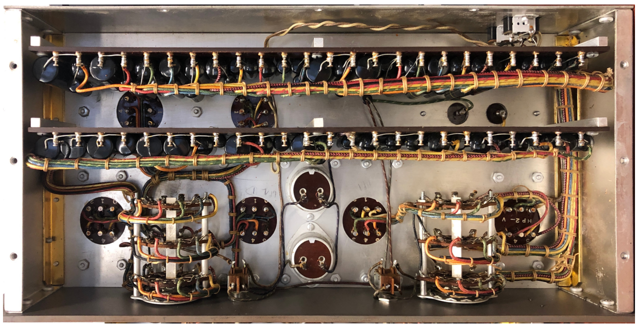

(b) SEF #2 Inside, bottom.

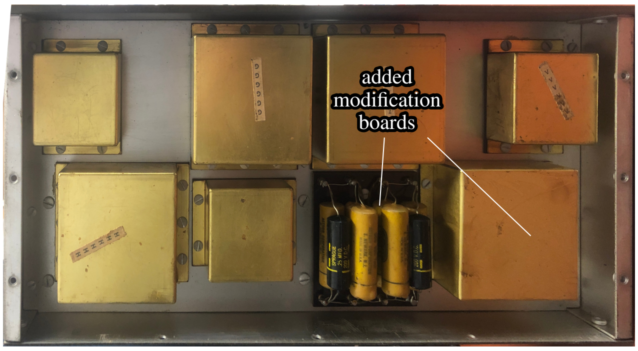

(c) SEF #2 Inside, top.

Figure 1: *Photographs of the front panel of Sound Effects Filter #1, and top and bottom of inside of Sound Effects Filter #2.*

ing, rather than the impedance bridging principle that more modern circuits typically use. The output is already loaded internally by the 560 Ω resistor R_t. and the circuit is designed to be driven by a 560 Ω resistive voltage source. Hence, we add a 560 Ω resistor R_{in} to the ideal voltage source v_{in} to represent this.

2.1. Circuit Modifications

The manual for the SEF includes pictures of the circuit, presumably taken at the date of manufacture. Comparing these pictures to the actual devices makes it clear the circuits were modified after that date. Externally, this discrepancy consists of two additional switches (visible in Fig. 1a) between the two original 11 position Mallory switches. Opening up each of the four unit allows us to reverse engineer this modification: the DPDT switches enable adding extra highpass and lowpass T sections. Some of the stock capacitors were visibly re-purposed to be part of the additional low pass stage, with a lead noticeable in the original picture missing in the current incarnation of the device. A new component replaces the missing capacitor in its original bundle. A generalized schematic of the device, updated from R. A. Lynn's original design to include this modification, is included in Fig. 2.

This modification is built with the same standards as the original units, with wire bundles being redone to include the new connections rather than being laid on top or left hanging. Where possible, it seems the same parts were used as for the original construction, with black Sprague capacitors alongside newer Astron Corporation-branded yellow ones seen on the additional board visible in Fig. 1c. Conversation with Peter Mauzey suggests the modification was implemented by RCA staff.[4]

Markings near SEF #1's switches, not found on the three other units, read "0," "100," "5700," and "∞." There is some evidence that Ussachevsky and others experimented with impedance mismatching throughout the Mark II to explore the timbral results. Ussachevsky wrote that "Because our equipment was mismatched, we deliberately made use of the distortions it produced and gave them musical value. It is amusing that later an article [20] was written discussing our use of mismatched impedance as a new phenomenon."[5] However, today all four units seem identical, and the modified input and termination resistances implied by these markings are not present, pointing to a process of experimentation where not all modificationss survive.

These modifications meaningfully connect technical decisions to artistic consequences, giving both circuit and music scholars an opportunity to know what mattered enough to the users and maintainers of the machine to install meticulous changes to the four units. Although this would not have been called circuit-bending [21] when it was implemented, it also motivates our use of low-level circuit modelling techniques such as WDFs, which support digital models of circuit-bending [22].

3. DERIVING COMPONENT VALUES

Some challenges of studying and modeling the SEF are that the schematics give only partial information, many component devices on the circuit are not labelled, and the device is too fragile and rare to desolder any components for measurement.

Luckily, the schematics include the termination resistor and all capacitor values. The schematics give "desired" capacitor values[6] and then the actual embodiments through the parallel combination of 1–4 capacitors. The reason for this is that capacitors are only manufactured at specific values—they would be using combinations of the values available to them to get as close to the desired values as possible. We will always use the "actual" value rather than the "desired" value in our calculations. These values are given in Tab. 1. The capacitances used in this circuit are from the set

$$\{0.022,\ 0.047,\ 0.05,\ 0.1,\ 0.15,\ 0.22,\ 0.25,\ 0.47,\ 0.5,\ 1.0\}\ \mu\text{F}.$$

[4] Email from Mauzey to Teboul, 3/26/2022

[5] Ussachevksy to Fahs, March 12, 1953. Rockefeller Foundation, RG 1.2, 200R, Box 296, Folder 2769, mentioned in email from Vandagriff to Werner, 12/12/2019.

[6] These are given to a high level of precision on the circuit diagram, and with lower precision in the documentation's capacitor embodiment discussion. We use the higher precision values. In three cases, the values differ in a way that cannot be ascribed to truncation or rounding. In those cases we use the higher precision values.

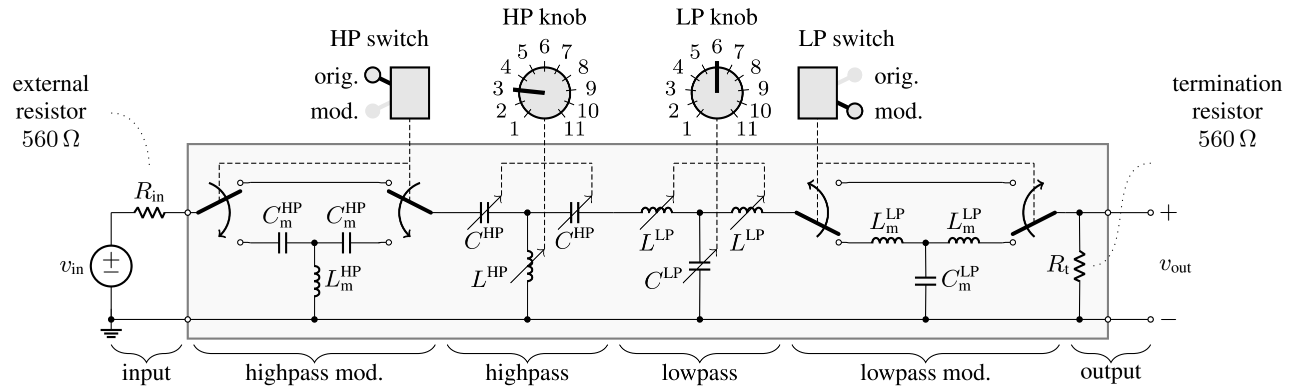

Figure 2: *Circuit diagram of the RCA Mark II Sound Effects Filter, including the modifications.*

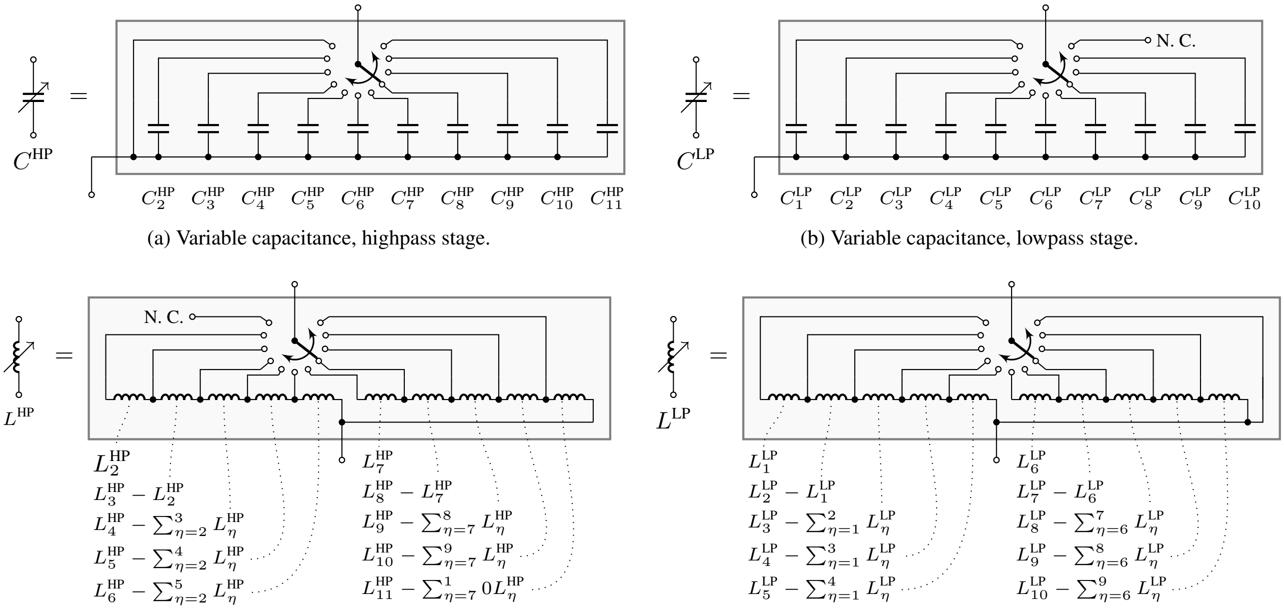

(a) Variable capacitance, highpass stage.

(b) Variable capacitance, lowpass stage.

(c) Variable inductance, highpass stage.

(d) Variable inductance, lowpass stage.

Figure 3: *Variable capacitances and inductances in the highpass and lowpass stages based on 11-position Mallory rotary switches.*

One might ask why, since they clearly had $0.15\ \mu\mathrm{F}$ capacitors available (e.g., C_4^{HP}, C_6^{HP}, C_9^{HP}, C_5^{LP}, C_7^{LP}, and C_{10}^{LP}), they embodied both the C_3^{HP} and C_4^{LP} capacitances as $1.0 + 0.1 + 0.05\ \mu\mathrm{F}$ rather than $1.0 + 0.15\ \mu\mathrm{F}$. This remains a mystery—perhaps just a matter of what was laying around on the workbench.

The inductor values, unfortunately, are not given directly. However, the schematics do give mechanical, material, and geometric properties of each inductor: most relevantly the number of wire turns and information on the toroidal inductor cores. As mentioned earlier, each inductor is not wrapped around a separate core; each one is realized with two multi-tapped inductors, where the appropriate core and tap is selected by the discrete control knobs. For the two types of inductor cores that are used, Arnold D-927156-3 and Arnold D-082168-3, tabulated values are available [23] that relate the number of wire turns N to the inductance L via a parameter called A_{L}. In [23], A_{L} is specified in units of mH-per-thousand-turns-squared, giving an expression for inductance L in henries of

$$L = N^2 A_{\mathrm{L}}/10^9. \tag{1}$$

All quantities and resulting inductances are given in Tab. 1.

For the three inductors $L_{\mathrm{m}}^{\mathrm{HP}}$ and $L_{\mathrm{m}}^{\mathrm{LP}}$ ($\times 2$) used in the circuit modification, no design documents or schematics are available. Therefore the core, turns ratio, etc., intended inductance, are all unknown. Luckily, we were able to obtain component values for these via direct measurement with an LCR meter.

3.1. Evaluation and Discussion

Here we study 3 related families of magnitude responses: curves given in the original schematics, measurements taken on the real device (SEF #2), and curves measured from a digital model made in LTspice. In the first case, only curves for $\ell_{\mathrm{HP}} = 1$, $\ell_{\mathrm{LP}} \in$

Table 1: *A summary of the design and characterization of the various stages in the SEF, including cutoff frequencies and their spacings, capacitor and inductor values. For each knob position, k and the cutoff frequency f_c are calculated using the "actual" (embodiment with 1–4 parallel caps) capacitor value and the "actual" (calculated via (1)) inductor value. For the Arnold toroidal MPP (molypermalloy powder) cores, A is model D-927156-3 and B is model D-082168-3.*

					capacitors				inductors				
stage	knob pos.	f_c (Hz)	distance to previous (semitones)	k (Ω)	name	desired (µF)	actual (µF)	embodiment (µF)	name	core	A_L $\left(\frac{\text{mH}}{\text{turns}^2}\right)$	turns (#)	actual (mH)
HP mod.	—	86.7	∞	564.6	C_m^{HP}	?	3.25	$1.0+1.0+1.0+0.25$	L_m^{HP}	?	?	?	518
highpass	1	0	——	——	"C_1^{HP}"	"∞"	——	——	"L_1^{HP}"	—	——	——	"∞"
	2	175	(12.1)	565.2	C_2^{HP}	1.62	1.6	$1.0+0.5+0.1$	L_2^{HP}	A	156	1280	255.6
	3	248	6.37	554.7	C_3^{HP}	1.16	1.15	$1.0+0.1+0.05$	L_3^{HP}			1065	176.9
	4	352	5.83	562.1	C_4^{HP}	0.81	0.8	$0.5+0.15+0.15$	L_4^{HP}			900	126.4
	5	497	5.85	562.3	C_5^{HP}	0.57	0.57	$0.47+0.1$	L_5^{HP}			760	90.11
	6	699	5.95	505.6	C_6^{HP}	0.406	0.4	$0.25+0.15$	L_6^{HP}	↓	↓	640	63.90
	7	1002	6.24	572.4	C_7^{HP}	0.283	0.272	$0.25+0.022$	L_7^{HP}	B	168	515	44.56
	8	1411	5.85	563.8	C_8^{HP}	0.2	0.2	$0.1+0.1$	L_8^{HP}			435	31.79
	9	2024	6.55	538.8	C_9^{HP}	0.142	0.15	0.15	L_9^{HP}			360	21.77
	10	2847	5.74	559.1	C_{10}^{HP}	0.1	0.1	0.1	L_{10}^{HP}			305	15.63
	11	3994	5.79	569.3	C_{11}^{HP}	0.071	0.069	$0.047+0.022$	L_{11}^{HP}	↓	↓	258	11.18
lowpass	1	175	——	563.4	C_1^{LP}	3.24	3.22	$1.0+1.0+1.0+0.22$	L_1^{LP}	A	156	1810	511.1
	2	245	5.82	563.5	C_2^{LP}	2.32	2.3	$1.0+1.0+0.25+0.05$	L_2^{LP}			1530	365.2
	3	350	6.18	565.2	C_3^{LP}	1.62	1.6	$1.0+0.5+0.1$	L_3^{LP}			1280	255.6
	4	499	6.20	557.3	C_4^{LP}	1.14	1.15	$1.0+0.1+0.05$	L_4^{LP}			1070	178.6
	5	703	5.99	562.1	C_5^{LP}	0.812	0.8	$0.5+0.15+0.15$	L_5^{LP}	↓	↓	900	126.4
	6	996	5.87	562.0	C_6^{LP}	0.567	0.57	$0.47+0.1$	L_6^{LP}	B	168	732	90.02
	7	1408	6.03	563.7	C_7^{LP}	0.402	0.4	$0.25+0.15$	L_7^{LP}			615	63.54
	8	1989	5.94	575.7	C_8^{LP}	0.284	0.272	$0.25+0.022$	L_8^{LP}			518	45.08
	9	2803	5.80	567.7	C_9^{LP}	0.2	0.2	$0.1+0.1$	L_9^{LP}			438	32.23
	10	3992	6.30	546.3	C_{10}^{LP}	0.142	0.15	0.15	L_{10}^{LP}	↓	↓	365	22.38
	11	∞	∞	——	"C_{11}^{LP}"	"0"	——	——	"L_{11}^{LP}"	—	——	——	"0"
LP mod.	—	4826	(3.28)	439.7	C_m^{LP}	?	0.15	0.15	L_m^{LP}	?	?	?	14.5

$\{1,\cdots,11\}$ and $\ell_{HP} \in \{1,\cdots,11\}$, $\ell_{LP} = 1$ are given. These curves were extracted from a photograph of the schematics[7] using the WebPlotDigitizer tool [24]. In the other cases, we also measure two other "sweeps," with $\ell_{HP} = 6$ and $\ell_{LP} = 6$, to show some characteristic narrow bandpass shapes that can be created with the SEF. Measurements on the real device were taken using a MOTU UltraLite mk4, which has $100\,\Omega$ of output impedance and $10\,\text{k}\Omega$ of input impedance [25], using a 1-minute long white Gaussian noise sequence sampled at $44.1\,\text{kHz}$, the same sequence used in our time-domain LTspice simulations. In both cases, Welch's method ($2^{12} = 4096$-sample-long Hann windows, 50% overlap) is used to find magnitude responses from measured noise responses.

Because of the input and output impedances of the MOTU, we use modified versions of R_{in} and R_t throughout:

$$\tilde{R}_{in} = R_{in} + 100\,\Omega = 660\,\Omega, \quad \tilde{R}_t = R_t || 10\,\text{k}\Omega \approx 530.3\,\Omega. \quad (2)$$

Overall, the match between the 3 families of curves is fairly good. However, there are some differences in the shape of the magnitude responses. For instance, we see slight differences in cutoff frequencies between the model and measurements/schematics, more pronounced ripples in the measured data than in the model, and some extra passband loss in the measured data that does not appear in the model and is not suggested by the schematics.

This can be attributed to non-ideal behavior of the inductors or capacitors or aging (at time of writing, almost 70 years) components whose values differ from the schematics. As well, there is no indication of whether the schematic magnitude responses are themselves measurements or idealizations.

[7]The curves derived from the schematics go all the way up to 0 dB, which is obviously incorrect, as the resistors form a -6 dB voltage divider even in the passband. Hence, we normalize all the schematic curves by subtracting $-20\log_{10}(R_t/(R_{in}+R_t)) \approx 6.02$ dB.

4. CONSTANT-k CIRCUIT DESIGN

Although it is not discussed in the schematics, the circuit appears to have been designed using the "constant-k" design procedure [26]. In constant-k filter design, a cascade is formed of two-port circuit blocks which all satisfy the relationship

$$k^2 = Z/Y, \quad (3)$$

where k and Z are impedances and Y is an admittance. Specifically, k is the (constant) characteristic impedance of the cascade considered as a transmission line, Z is the impedance of its series aspect, and Y is the admittance of its shunt aspect.

Image impedance for symmetrical sections, which are the only ones used in this filter, are identical from each of the two ports.

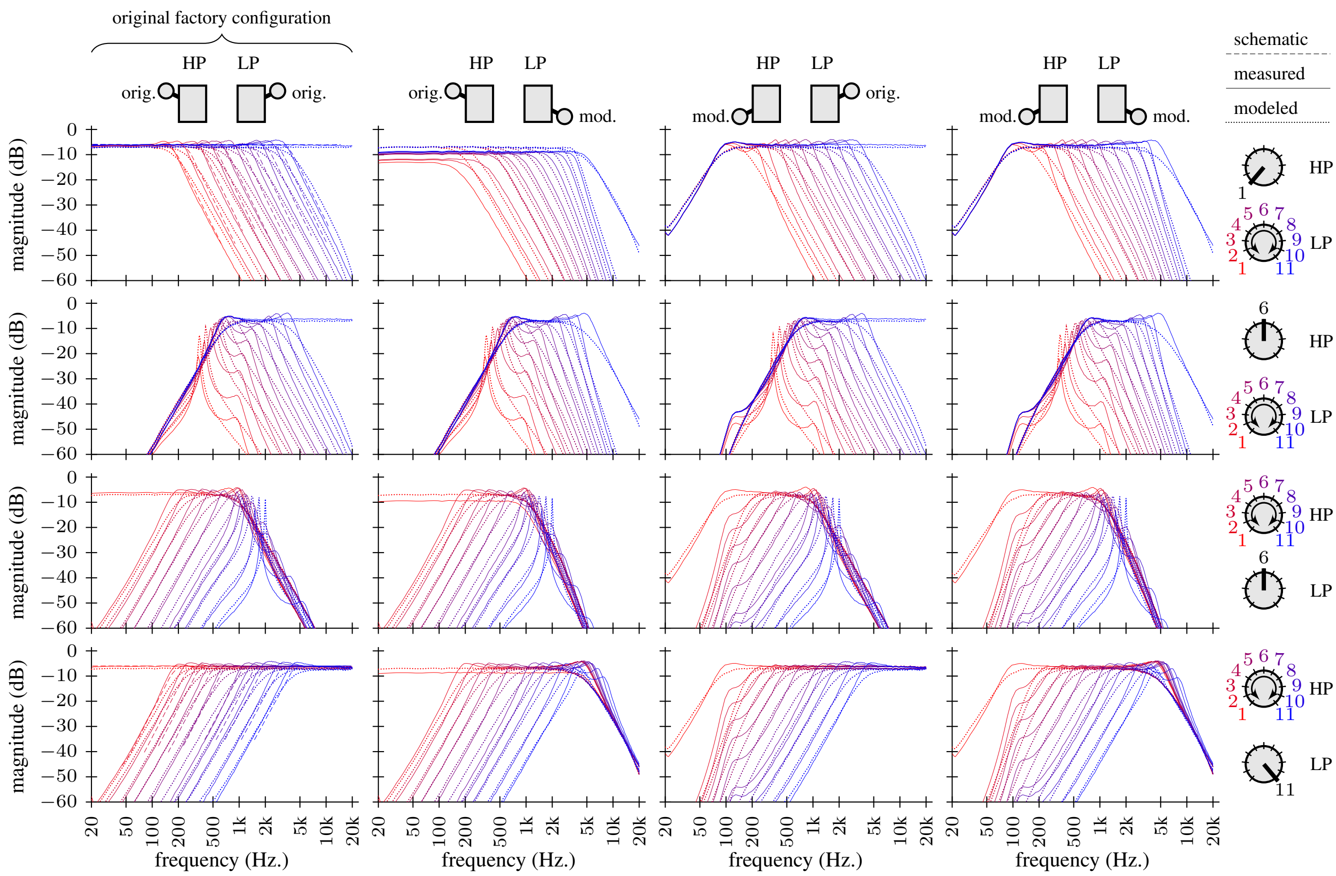

Figure 4: *Magnitude responses.*

Image impedance (Z_{im}) can be calculated from the short-circuit (Z_{sc}) and open-circuit (Z_{oc}) impedances as

$$Z_{\text{im}} = \sqrt{Z_{\text{sc}} Z_{\text{oc}}}. \tag{4}$$

Z_{sc} and Z_{oc} are found by short-circuiting (resp. open-circuiting) one port and calculating the input impedance at the other port.

A overview of the topology, Z_{sc}, Z_{oc}, Z_{im}, cutoff frequency (in radians) $\omega_{\text{c}} = 2\pi f_{\text{c}}$, and inductor and capacitor design equations for generic, highpass, and lowpass "T" sections is shown in Tab. 2. A typical way to do a constant-k design is to define a k, choose desired lowpass and highpass cutoff frequencies, then choose the inductor and capacitor values according to the design equations. Using the given, derived, and measured capacitor and inductor values from §3 and (3) gives a value of k for each stage, as shown in Tab. 1. We can see that each stage has a k of very nearly $560\,\Omega$. Small deviations are attributable to quantification concessions in capacitor selection and integer turn numbers used on the inductors. Since this is the stated design load of the circuit, this demonstrates that it was designed using constant-k principles.

5. WAVE DIGITAL FILTER MODEL

Having found the circuit topology and suitable component values, we can now derive a real-time digital model using the Wave Digital Filter (WDF) approach [22, 27].

We start by deciding how to handle the switches. It is possible to handle switches as ideal linear elements, but this requires grouping them all together at the root of the WDF tree, which leads to a quite complex topology [22, 28]. Another option is approximating each switch as two resistors: a tiny one (closed connection) and a huge one (open connection). This leads to a somewhat complex topology involving bridged-T networks [29]. For simplicity, we instead only treat the case where the modifications are engaged. To disengage a modification, we just adjust the values of C_{m}^{HP} and L_{m}^{HP} (resp. C_{m}^{LP} and L_{m}^{LP}) to have extremely low (resp. high) cutoffs, using the constant-k design equations in Tab. 2.

Using this strategy, we draw a circuit graph, shown in Fig. 5, where each of the 10 electrical nodes in Fig. 2 corresponds to a graph node a–j and each electrical component (treating v_{in} and $\tilde{R}_{\text{in}}$ together as a resistive voltage source) corresponds to a graph edge.

We then search for "split components," shown in Fig. 6a, identifying series ($\mathcal{S}$), parallel ($\mathcal{P}$), and "rigid" ($\mathcal{R}$) connections in the graph. Because of our modeling strategy w.r.t. switches, we have ended up with a separated graph that has no "rigid" connections, which would require special techniques [22, 29].

Selecting the resistive voltage source $v_{\text{in}} + \tilde{R}_{\text{in}}$ as the root[8], we can then create an SPQR (series (S), parallel (P), "singular"

[8]Typically, if there is are one [27] or more [22, 28, 29] non-adaptable elements, they would be selected as the root of the WDF tree. We have no non-adaptable elements, so our choice is arbitrary.

Table 2: *Generic, lowpass, and highpass symmetrical constant-k T-section schematics and design equations.*

type	Z_1	Z_2	circuit	$Z_{\mathrm{im}}(s)$	$Z_{\mathrm{im}}(0)$	ω_{c} (rad.)	$Z_{\mathrm{im}}(\omega_{\mathrm{c}})$	$Z_{\mathrm{im}}(\infty)$	L (H)	C (F)
generic	Z_1	Z_2	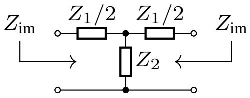	$\sqrt{\frac{Z_1}{2}\left(Z_1+4Z_2\right)}$	——	——	——	——	——	——
highpass (HP)	$\frac{1}{Cs}$	Ls	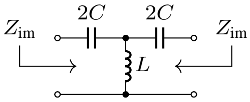	$\sqrt{\frac{1+4CLs^2}{2C^2s^2}}$	$\infty\mathrm{j}$	$\frac{1}{2}\sqrt{\frac{1}{CL}}$	0	$\sqrt{2\frac{L}{C}}$	$\frac{k}{2\sqrt{2}\omega_{\mathrm{c}}}$	$\frac{\sqrt{2}}{k\omega_{\mathrm{c}}}$
lowpass (LP)	Ls	$\frac{1}{Cs}$	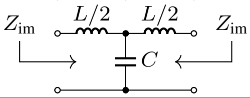	$\sqrt{\left(\frac{L}{C}\right)\frac{LCs^2+4}{2}}$	$\sqrt{2\frac{L}{C}}$	$2\sqrt{\frac{1}{CL}}$	0	$\infty\mathrm{j}$	$\frac{\sqrt{2}k}{\omega_{\mathrm{c}}}$	$\frac{2\sqrt{2}}{k\omega_{\mathrm{c}}}$

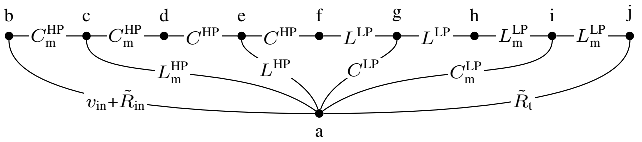

Figure 5: *Circuit graph.*

(Q), and "rigid" (R)) tree structure [30], shown in Fig. 6b, that is isomorphic to the separated graph.

This SPQR tree is isomorphic to a WDF structure, shown in Fig. 6c. Each block in this structure has a number of ports with an associated port resistance, which is calculated by "adapting" each port, working "up" the tree starting at the leaves. It also indicates an explicit sequence of calculations that happens in three phases: propagation of waves up the tree, calculation at the root, and propagation of waves down the tree. For more information, see [22,27]. We can also see the structure underlying this WDF by redrawing the original circuit, as shown in Fig. 6d.

The WDF is built in the Faust programming language using the "WDmodels" library [31], which allows a WDF tree to be specified in Faust, which can then compile to a number of targets. In particular, we compiled our WDF model to a Pure Data external.[9]

Our code begins by declaring the controls as well as the capacitor and inductor values. These are called in the component definitions, which convert the WDF shown in Fig. 6 into a network of adds, multiplies, and delays. The key line specifying our tree, which gives a sense of the usage of WDmodels is:

```
tree = v_in : (wd.series :
 (c_HPm1, (wd.parallel :
  (l_HPm, (wd.series :
   (c_HPm2, (wd.series :
    (c_HP1, (wd.parallel :
     (l_HP, (wd.series :
      (c_HP2, (wd.series :
       (l_LP1, (wd.parallel :
        (c_LP, (wd.series :
         (l_LP2, (wd.series :
          (l_LPm1, (wd.parallel :
           (c_LPm, (wd.series :
            (l_LPm2, r_T)
             ))))))))))))))))))))))));
```

[9] Using the method in [32], this and models of related CMC equipment form the basis for a partial digital model of some historical RCA Mark II configurations in Pure Data, derived from the original documentation developed by R. A. Lynn at RCA. Code will be released under a noncommercial license mid-2022, alongside compositions for this system.

As a practical matter, to compensate for gain loss, a $2\times$ multiplier (inverse of the voltage divider ratio $\frac{R_{\mathrm{t}}}{R_{\mathrm{in}}+R_{\mathrm{t}}}=\frac{560}{560+560}=\frac{1}{2}$) is also added to the output, to get a baseline passband gain of 1.

6. EXTENSIONS

As mentioned earlier, circuit modifications were a part of the artistic tradition of using the SEF. However, today the filters' fragility means that they can no longer be modified. However, now that we have a suitable digital model, we can implement a number of extensions to the basic circuit. First of all, it is possible to "circuit bend" [21] the model by changing any component value away from its original design, guided by intuition and pleasing sonic results.

By deliberately mismatching the input and termination resistaces, as suggested by Ussachevsky's letter and [20], musically useful vocal-formant-like resonances can be introduced into the filter magnitude response. An especially useful configuration is reducing the input impedance R_{in} while increasing the termination impedance R_{t}. An example is shown in Fig. 7, which shows the magnitude response for $\ell_{\mathrm{HP}}=3$, $\ell_{\mathrm{LP}}=9$, with both the HP and LP modification stages engaged, but mismatching the impedances to the values shown on the front panel of SEF #1 (recall Fig. 1a). Note that as the impedances get more mismatched, the resonances become more dramatic.

It is also possible to use the findings from our reverse engineering efforts to introduce more deliberate modifications. Knowing the constant-k design equations (Tab. 2), it is a simple matter to change the fixed frequency controls into continuously variable frequency controls. Similarly, we can extend the circuit to have any number of fixed or variable highpass and lowpass stages, to obtain steeper cutoffs. It would also be a simple matter to augment the circuit with other known building blocks that are compatible with constant-k designs, such as allpass, bandpass, or bandstop.

A common practice with the SEF is to "cross over" the HP and LP stages (setting $\ell_{\mathrm{LP}}<\ell_{\mathrm{HP}}$) to get narrow bandpass filters. An undesirable side effect of this is significant signal loss. A practical extension that can be devised is a simple gain compensation based on normalizing against the magnitude response peak or the impulse response energy at any setting.

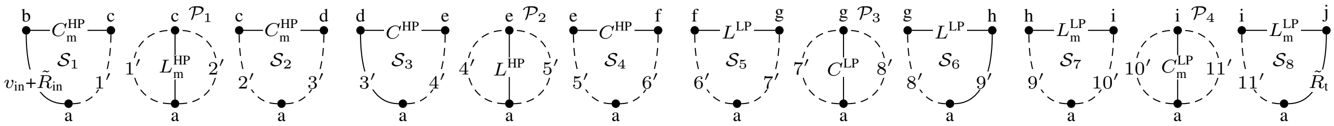

(a) First a search for split components yields a graph separated into series ($\mathcal{S}$) and parallel ($\mathcal{P}$) components connected by (dotted) virtual edges.

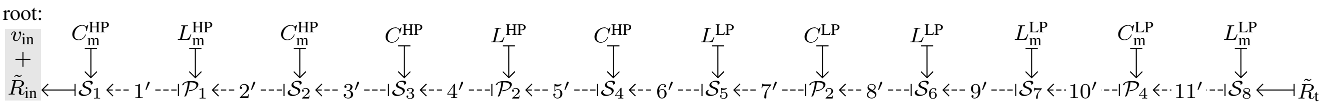

(b) Assigning the resistive voltage source as the root, this is converted to a SPQR tree structure, where arrows point "up" the tree.

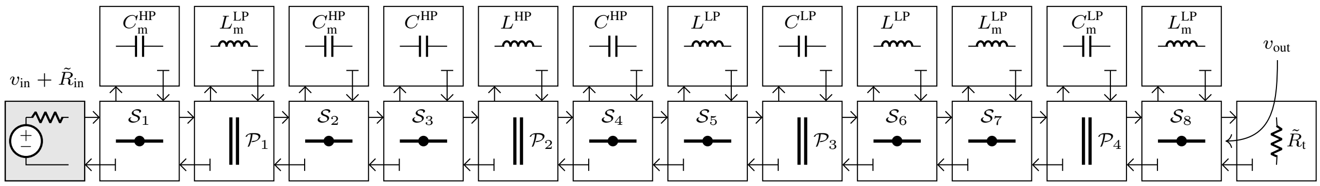

(c) This structure is now isomorphic to a WDF structure.

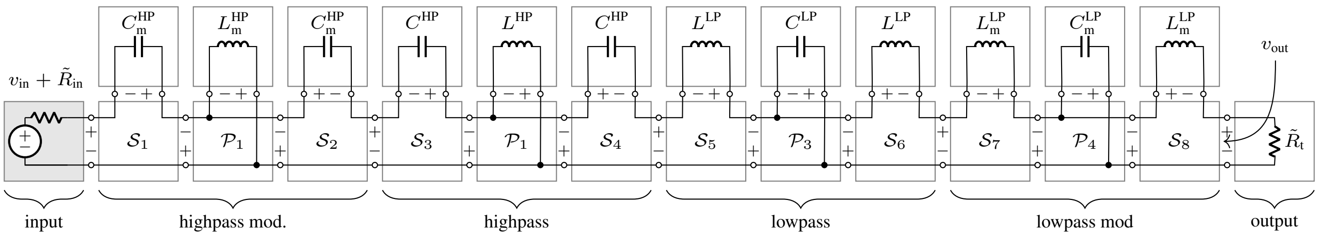

(d) This structure can also be seen by rearranging the original circuit to highlight its topology.

Figure 6: *The process of turning the circuit graph of Fig. 5 into a WDF that models the RCA Mark II Sound Effects Filter.*

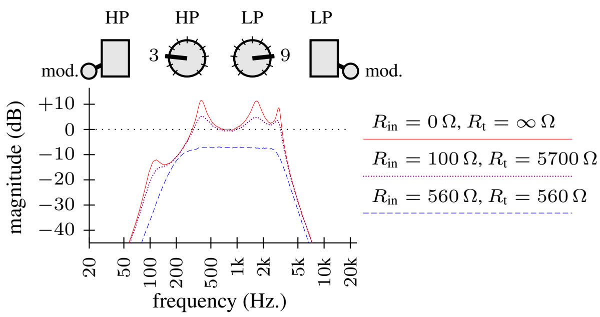

Figure 7: *Magnitude response ripples via impedance mismatching.*

7. CONCLUSION

We have analyzed the design and behavior of the RCA Mark II synthesizer's Sound Effects Filter, reconciling differences between the schematics and modifications performed to the device, and proposed a number of extensions. A Wave Digital Filter model was created in Faust, using the WDmodels library, that captures the basic measured behavior. Future work may investigate non-ideal inductor and capacitor models for improved accuracy.

Examining the technical decisions materialized in the circuits and building a model for continued use provides a new avenue for understanding the machine and its context. Post-installation modifications, such as the presence of added stages, necessitates the use of reverse engineering techniques [33]. For instance, although we were able to identify that the circuit is based around a constant-k design, without access to the original engineer, some questions cannot be answered. This initial study of the Mark II's circuits shows that it can be critical that archival materials be compared to design decisions and modifications in actual circuit embodiments.

As part of a larger effort to reckon with the cultural and symbolic importance of the RCA Mark II, while also undoing the technical and cultural gate-keeping that made it inaccessible to most [34] (by making a model widely available), this paper is a first step in developing a material history of the hardware holdings at the CMC. Our analysis helps us understand what, sonically in addition to technically, the large socio-technical system of the RCA Mark II made possible at this nexus of non- and for-profit artistic and scientific research within the wider context of American cold-war era information theory [3, 4, 6, 35].

8. ACKNOWLEDGMENTS

Thank you to Emily Lavins and Nick Patterson for assistance with the CMC archive, to Dirk Roosenburg for their WDF modeling library, and to Rachel Vandagriff for help sourcing the Ussachevsky quote. Ezra Teboul thanks Seth Cluett, Kurt James Werner, Pril Smiley, Alice Shields, Ricardo Dal Farra, Andres Lewin-Richter, Alcides Lanza, and Peter Mauzey for research and logistical help.

9. REFERENCES

[1] A. C. García and A. P. Yuste, "The role of the White House in the establishment of a governmental radio monopoly in the United States: The case of the Radio Corporation of America," in *Proc. 2nd Region 8 IEEE Conf. Hist. Commun.*, Madrid, Spain, Nov. 2010.

[2] H. F. Olson and H. Belar, "Electronic music synthesizer," *J. Acoust. Soc. Am.*, vol. 27, no. 3, pp. 595–612, May 1955.

[3] M. Brody, "The enabling instrument: Milton Babbitt and the RCA synthesizer," *Contemporary Music Rev.*, vol. 39, no. 6, pp. 776–794, Nov. 2020.

[4] M. Babbitt, "An introduction the the RCA synthesizer," *J. Music Theory*, vol. 8, no. 2, pp. 251–265, Winter 1964.

[5] R.J. Gluck, "The Columbia–Princeton Electronic Music Center: Educating international composers," *Comput. Music J.*, vol. 31, no. 2, pp. 20–38, June 2007.

[6] R. Vandagriff, "The pre-history of the Columbia-Princeton Electronic Music Center," talk presented at the "Alternative Hist. Electron. Music" symp., London, UK, Apr. 2016.

[7] E. Lemmon, "The impact of institutional support on artistic research and creation: The Columbia-Princeton Electronic Music Center and the RCA Mark-II," in *Proc. Int. Comput. Music Conf.*, New York, NY, June 2019.

[8] A. Battaglia, "Circuits in the grid: The Columbia-Princeton Electronic Music Center in Harlem in the '50s, '60s & '70s," Dec. 2012, `https://iaspm-us.net/jpms-online-popiaspm-us-sounds-of-the-city-issue-andy-battaglia/`.

[9] P. McCray, *Making Art Work: How Cold War Engineers and Artists Forged a New Creative Culture*, MIT Press, Cambridge, MA, 2020.

[10] A. J. Wolfe, *Competing with the Soviets: Science, Technology, and the State in Cold War America*, John Hopkins Uni. Press, Baltimore, MD, 2012.

[11] H. F. Olson, H. Belar, and J. Timmens, "Electronic Music Synthesis," *J. Acoust. Soc. Am.*, vol. 32, no. 3, pp. 311–319, 1960.

[12] H. F. Olson, *Music, Physics and Engineering*, Courier Corp., 1967.

[13] H. F. Olson and H. Belar, "Music synthesizer," U.S. Patent #2,8555,816, Oct. 14, 1958.

[14] H. F. Olson, "Electronic music synthesis for recordings," *IEEE Spectr.*, vol. 8, no. 4, pp. 18–30, Apr. 1971.

[15] N. Patterson, "The archives of the Columbia-Princeton Electronic Music Center," *Notes: Quarterly J. Music Library Assoc.*, vol. 67, no. 3, pp. 483–502, Mar. 1968.

[16] S. Cluett, "Preserving hardware history: Archiving the studios at Columbia University," *Array, J. ICMA*, pp. 15–21, 2002.

[17] S. Canazza, F. Avanzini, M. Novati, and A. Roda, "Active preservation of electrophone musical instruments. the case of the 'Liettizzatore' of 'Studio Di Fonologia Musicale' (RAI, Milano)," in *Proc. Sound Music Comput. Conf.*, Padova, Italy, Jan. 2011.

[18] Y. Nakai, *Reminded by the Instruments: David Tudor's Music*, Oxford Uni. Press, Oxford, UK, 2021.

[19] K. J. Werner and E. J. Teboul, "Analyzing a unique pingable circuit: The gamelan resonator," in *Proc. 151st Audio Eng. Soc. Conv.*, New York, NY, 2021, Paper #10542.

[20] A. Berger, "Music written for the (tape) recorder," *New York Herald Tribune*, Oct. 26 1952.

[21] Q. R. Ghazala, "The folk music of chance electronics: Circuit-bending the modern coconut," *Leonardo Music J.*, vol. 14, pp. 97–104, 2004.

[22] K. J. Werner, *Virtual analog modeling of audio circuitry using wave digital filters*, Ph.D. diss., Stanford Univ., 2016.

[23] W. T. McLyman, *Magnetic Core Selection for Transformers and Inductors: A User's Guide to Practice and Specifications*, CRC Press, Boca Raton, FL, 1997, 2nd ed.

[24] A. Rohatgi, "WebPlotDigitizer: Version 4.5," 2021, `https://automeris.io/WebPlotDigitizer`.

[25] MOTU, "UltraLite-mk4 user guide," 2016, `https://s3.amazonaws.com/motu-www-data/manuals/proaudio/UltraLite-mk4_User_Guide.pdf`.

[26] G. A. Campbell, "Physical thory of the electric wave-filter," *Bell Syst. Tech. J.*, vol. 1, no. 2, pp. 1–32, Nov. 1922.

[27] A. Fettweis, "Wave digital filters: Theory and practice," *Proc. IEEE*, vol. 74, no. 2, pp. 270–327, Feb. 1986.

[28] K. J. Werner, W. R. Dunkel, and F. G. Germain, "A computational model of the Hammond organ vibrato/chorus using wave digital filters," in *Proc. 19th Int. Conf. Digital Audio Effects*, Brno, Czech Republic, Sept. 2016, pp. 271–278.

[29] K.J. Werner, A. Bernardini, J.O. Smith III, and A. Sarti, "Modeling circuits with arbitrary topologies and active linear multiports using wave digital filters," *IEEE Trans. Circuits Syst. I: Reg. Papers*, vol. 65, no. 12, pp. 4233–4246, Dec. 2018.

[30] D. Fränken, J. Ochs, and K. Ochs, "Generation of wave digital structures for networks containing multiport elements," *IEEE Trans. Circuits Syst. I: Reg. Papers*, vol. 52, no. 3, pp. 586–596, Mar. 2005.

[31] D. Roosenburg, E. Stine, R. Michon, and J. Chowdhury, "A wave digital filter modeling library for the Faust programming language," in *Proc. 18th Sound Music Comput. Conf.*, Virtual, June–July 2021, pp. 24–30.

[32] E. J. Teboul, *A method for the analysis of handmade electronic music as the basis of new works*, Ph.D. diss., Rensselaer Polytech. Inst., Troy, NY, July 2020.

[33] E. J. Chikofsky and J. H. Cross, "Reverse engineering and design recovery: a taxonomy," *IEEE Softw.*, vol. 7, no. 1, pp. 13–17, Jan. 1990.

[34] T. Rodgers, "Tinkering with cultural memory: Gender and the politics of synthesizer historiography," *Feminist Media Hist.*, vol. 1, no. 4, pp. 5–30, Oct. 2015.

[35] R. Maconie, "Care to listen: Milton Babbitt and information science in the 1950s," *Tempo*, vol. 65, no. 258, pp. 20–36, Oct. 2011.